Imaging chromophores with undetectable fluorescence by stimulated emission microscopy

Wei Min[1]*, Sijia Lu[1]*, Shasha Chong[1], Rahul Roy[1], Gary R. Holtom[1] & X. Sunney Xie[1]

Fluorescence, that is, spontaneous emission, is generally more sensitive than absorption measurement, and is widely used in optical imaging[1,2]. However, many chromophores, such as haemoglobin and cytochromes, absorb but have undetectable fluorescence because the spontaneous emission is dominated by their fast non-radiative decay[3]. Yet the detection of their absorption is difficult under a microscope. Here we use stimulated emission, which competes effectively with the nonradiative decay, to make the chromophores detectable, and report a new contrast mechanism for optical microscopy. In a pump–probe experiment, on photoexcitation by a pump pulse, the sample is stimulated down to the ground state by a time-delayed probe pulse, the intensity of which is concurrently increased. We extract the miniscule intensity increase with shot-noise-limited sensitivity by using a lock-in amplifier and intensity modulation of the pump beam at a high megahertz frequency. The signal is generated only at the laser foci owing to the nonlinear dependence on the input intensities, providing intrinsic three-dimensional optical sectioning capability. In contrast, conventional one-beam absorption measurement exhibits low sensitivity, lack of three-dimensional sectioning capability, and complication by linear scattering of heterogeneous samples. We demonstrate a variety of applications of stimulated emission microscopy, such as visualizing chromoproteins, non-fluorescent variants of the green fluorescent protein, monitoring *lacZ* gene expression with a chromogenic reporter, mapping transdermal drug distributions without histological sectioning, and label-free microvascular imaging based on endogenous contrast of haemoglobin. For all these applications, sensitivity is orders of magnitude higher than for spontaneous emission or absorption contrast, permitting non-fluorescent reporters for molecular imaging.

The phenomenon of stimulated emission was first described by Einstein in 1917 (ref. 4). An atom or molecule in its excited state can be stimulated down to the ground state by an incident light field, resulting in the creation of a new coherent photon identical to those in the original incident field. This process only occurs when the frequency of the incident field matches the transition energy. Stimulated emission was later used as a fundamental principle for light amplification in the laser[5]. The depopulation aspect of stimulated emission has been used for population dumping from excited states[6], super-resolution fluorescence microscopy[7], and fluorescence lifetime imaging[8]. Here we use the light-amplification aspect of stimulated emission as a contrast mechanism for highly sensitive imaging of chromophores that have undetectable fluorescence.

Such chromophores have very short-lived excited states with much faster non-radiative decay rates than their spontaneous emission rates. As a result, their feeble fluorescence is overwhelmed by backgrounds, such as stray light, solvent Raman scattering, and detector dark counts. Our solution to this problem is to conduct a dual-beam experiment to interrogate the short-lived excited state by stimulated emission, which can compete with the non-radiative decay under a strong enough stimulating field (Fig. 1a). The resulting 'amplification' of the stimulation beam can then be detected in the presence of the background signals.

Considering the optical excitation at frequency ω_{01} (Fig. 1a), the absorption cross-section $\sigma_{\mathrm{abs}[0\rightarrow1]}$ is about $10^{-16}\,\mathrm{cm}^2$ for a single chromophore at room temperature[2,9]. As shown in Fig. 1b, under a tightly focused laser beam with a beam waist area of S ($\sim10^{-9}\,\mathrm{cm}^2$), the integrated intensity attenuation of the excitation beam $\Delta I_E/I_E$ is proportional to the ratio between $\sigma_{\mathrm{abs}[0\rightarrow1]}$ and S:

$$\Delta I_E/I_E = -N_0\sigma_{\mathrm{abs}[0\rightarrow1]}/S \qquad (1)$$

where N_0 is the number of molecules in the ground state. For a single chromophore, $\Delta I_E/I_E$ is of the order of 10^{-7}. Such small attenuation cannot be detected by conventional absorption microscopy. We note that single-molecule absorption was previously achieved in cryogenic temperatures using a frequency-modulation method[10], which is, however, difficult to implement at room temperature because of the broad molecular absorption linewidth. Moreover, absorption measurement is often complicated by scattering when imaging biological specimens. Instead of detecting direct absorption, here we detect the stimulated emission followed by the excitation of the molecule.

According to Einstein[4], the molecular cross-section σ_{stim} for stimulated emission is comparable to σ_{abs}, because of microscopic reversibility. Unlike the absorption that results in attenuation, the stimulation beam will experience an intensity gain after interacting with the molecules:

$$\Delta I_S/I_S = +N_2\sigma_{\mathrm{stim}[2\rightarrow3]}/S \qquad (2)$$

where N_2 is the number of excited molecules transiently probed by the stimulation pulses (Fig. 1b). For a single chromophore, $\Delta I_S/I_S$ is also $\sim10^{-7}$. Without special techniques, such a small signal would again be buried in the noise ($\sim$1%) of the stimulation beam.

To overcome this noise problem in detecting stimulated emission, we implemented a high-frequency (>1 MHz) phase-sensitive detection technique. In so doing, the laser intensity fluctuation, which occurs primarily at low frequency (kilohertz to direct current), can be circumvented, as has been previously applied in other spectroscopic[11] and recently stimulated Raman scattering microscopy[12] and two-photon absorption microscopy[13]. In the scheme shown in Fig. 1b and c, the intensity of the excitation beam is modulated at 5 MHz, and this creates a modulation of the stimulated emission signal at the same frequency, because only when the excitation beam is present can the gain of the stimulation beam occur. Such an induced modulation signal can then be sensitively extracted by a lock-in amplifier referenced

[1]Department of Chemistry and Chemical Biology, Harvard University, Cambridge, Massachusetts 02138, USA.
*These authors contributed equally to this work.

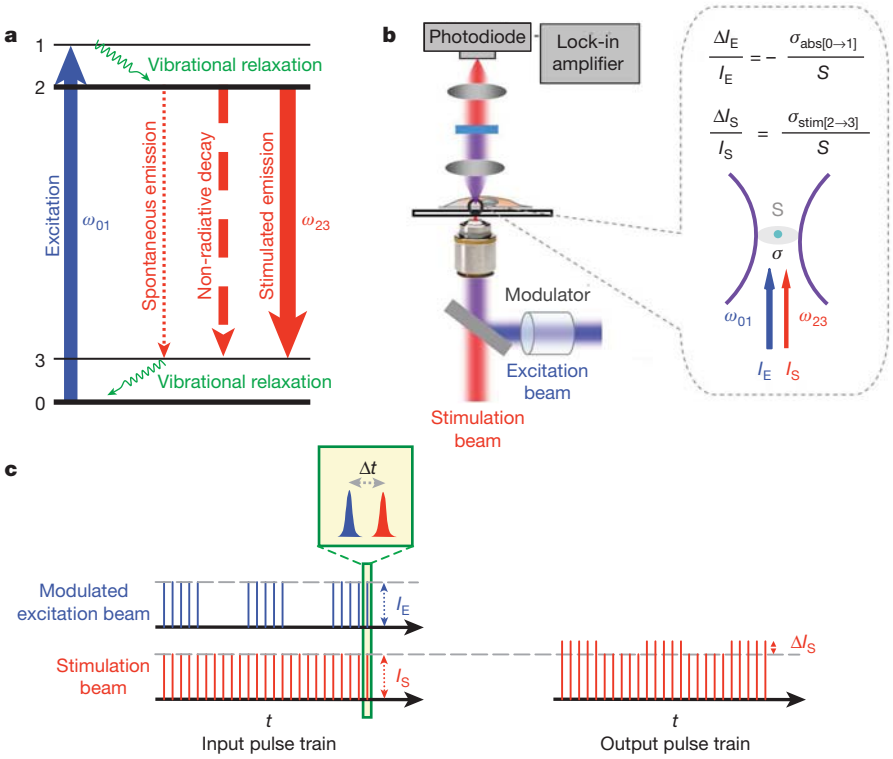

Figure 1 | Principles of stimulated emission microscopy. a, Energy diagram of spontaneous emission, non-radiative decay and stimulated emission processes for a typical four-level energy system. Non-radiative decay dominates spontaneous emission for chromophores with undetectable fluorescence. However, when the stimulation field is designed to have the correct energy and timing, the stimulated emission can compete with non-radiative decay and become the dominating decay pathway. **b**, Stimulated emission microscopy. The incident excitation and delayed stimulation pulse trains are spatially overlapped and focused onto the common focal spot in the sample. A modulator switches the intensity of the excitation beam on and off at 5 MHz. The spectrally filtered stimulation beam is detected by a large-area photodiode, and demodulated by a lock-in amplifier to create the image contrast while raster scanning the collinear exciting and stimulating beams. The relative energy gain or loss of the stimulation and excitation beam, respectively, for a single chromophore at the laser focus (area of S), is given by the equations (inset). **c**, Principles of high-frequency modulation. As the intensity of the excitation beam is modulated on and off over time, the corresponding stimulated emission signal is also modulated at the same frequency. The stimulation pulses are made to lag behind the excitation pulses by an appropriate Δt.

to this high frequency. In this way, the stimulated emission signal can be detected against the laser noise with orders-of-magnitude higher amplitude. In contrast, it is difficult to implement such a modulation scheme for high-sensitivity one-beam absorption measurement[11].

Specifically, we use a ~200-femtosecond (fs) (full-width at half-maximum, FWHM) pulse train for excitation, and another ~200-fs pulse train for stimulation. The time delay between these two pulse trains is chosen to be ~300 fs (Fig. 1c), which is shorter than the excited-state lifetime (sub-picosecond, ps) of the chromophores. This delay also eliminates contributions from other instantaneous optical processes, such as two-photon absorption[13], cross-phase modulation and stimulated Raman scattering[12].

We conduct the experiment under a non-saturating condition of the four-level system (Fig. 1a). Under this condition, N_2 in equation (2) originates from a linear excitation: $N_2 \propto N_0 I_E \sigma_{abs[0\to1]}/S$. This relation, together with equation (2), indicates that the final signal ΔI_S is linearly dependent on both I_E and I_S:

$$\Delta I_S \propto N_0 I_E I_S (\sigma_{abs[0\to1]}/S)/(\sigma_{stim[2\to3]}/S) \quad (3)$$

The overall quadratic power dependence, as experimentally demonstrated (Fig. 2a), would allow three-dimensional optical sectioning, as in many other multi-photon techniques[14,15]. Such dependence also confirms the non-saturation condition within the intensity range used. Moreover, it offers, in principle, a spatial resolution twice as high (in spatial frequency) as in conventional fluorescence microscopy.

Figure 2b shows the stimulated emission signal as a function of the time delay between the excitation and stimulation pulses. In the pump–probe experiment, the signal could arise from ground-state recovery, excited-state absorption or stimulated emission. Ground-state recovery is avoided here by the large Stokes shift of stimulation beam from the molecular absorption band. Excited-state absorption is negligible compared to stimulated emission, on the basis of the observed intensity increase of the stimulation beam, consistent with a study of fluorescence quenching in stimulated emission depletion microscopy[16]. The initial rise in Fig. 2b is due to vibrational relaxation from level 1 to level 2 (Fig. 1a), while the subsequent decay indicates the short excited-state lifetime (~0.6 ps) of level 2, which underlies the undetectable fluorescence. Such a short lifetime also reduces the probability of going into the triplet state, effectively protecting the molecule from photo-bleaching. The stimulated emission spectrum (Fig. 2c), recorded by tuning the wavelength of the stimulated beam, is also in agreement with the reported emission spectrum of crystal violet in glycerol[17], in which the high viscosity increases the fluorescence quantum yield.

Figure 2d shows that the stimulated emission signal depends linearly on analyte concentration, as predicted by equation (3). This allows straightforward quantitative analysis. The limit of detection is ~60 nM for crystal violet with 1 s integration time. This sensitivity effectively corresponds to a few (<5) molecules in focus, which has surpassed the detection limit recently reported for stimulated Raman scattering microscopy[12] by orders of magnitude because of the strong electronic transition. The ultimate sensitivity would be achieved under the condition of saturated excitation but near-saturated stimulation, and is fundamentally determined by the shot noise of the stimulation beam ($\Delta I_S/I_S \approx 10^{-7.5}$ for ~1 mW, averaged over 1 s).

As the first biological application, we imaged distributions of chromoproteins in live *Escherichia coli* cells. Genetically encodable

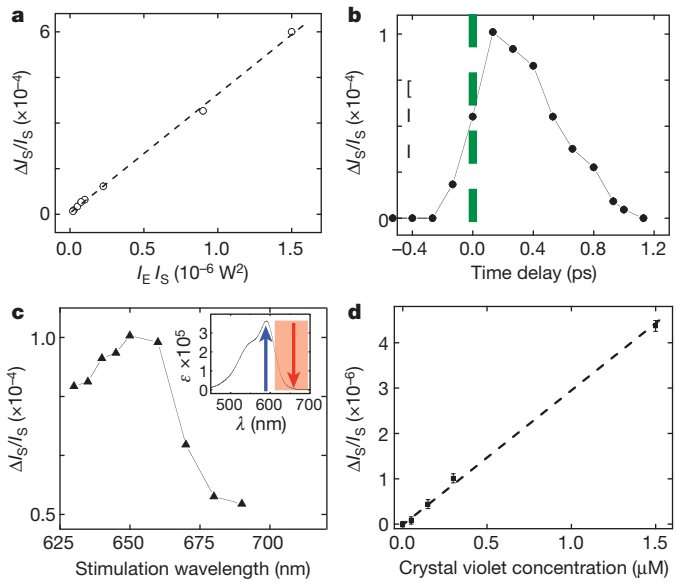

Figure 2 | Characterizations of stimulated emission microscopy. **a**, Stimulated emission signal from 30 μM crystal violet/water solution is proportional to the product of excitation beam power, I_E, and stimulation beam power, I_S. **b**, Stimulated emission signal as a function of time delay between the excitation (590 nm) and the stimulation (660 nm) pulses. The decay of the signal (~0.6 ps) reflects the short excited-state lifetime. The FWHM of the pulses is ~200 fs. **c**, The measured stimulated emission spectrum is in agreement with the reported fluorescence spectrum of crystal violet in glycerol solution[16]. The 590 nm excitation is fixed while the stimulation wavelength is scanned by tuning the other optical parametric oscillator wavelength. A time delay of 0.3 ps is used. Inset, the absorption spectrum of crystal violet in water. ε, Molar extinction coefficient. **d**, The stimulated emission signal scales linearly with crystal violet concentration in aqueous solution. Continuous flow of the sample is used to replenish molecules. Wavelengths are 590 nm and 660 nm for excitation and stimulation beam, respectively, and the time delay is 0.3 ps. Error bars show 1 s.d. of the signals from a 30 s recording. The detection limit was determined to be 60 nM with a signal-to-noise ratio of 1:1 (Supplementary Fig. 3). The excitation and stimulation beam intensities at the focus are 0.2 mW (~0.14 MW cm^{-2}) and 1 mW (~0.70 MW cm^{-2}), respectively. For 1 s time constant at the lock-in amplifier, a relative signal of 10^{-7} for $\Delta I_S/I_S$ can be detected.

chromoproteins, such as gtCP[18] and cjBlue[19], are naturally existing variants of green fluorescent proteins[20]; they absorb light but do not fluoresce. When the gene encoding gtCP is expressed in *E. coli* cells, tetrameric gtCP can be clearly seen residing homogeneously inside the cytoplasm by stimulated emission microscopy (Fig. 3a and b). Similarly, the distribution of another chromoprotein, cjBlue, can be imaged (Fig. 3c and d). Unlike gtCP, which is expressed in most cells, cjBlue is expressed in a fraction of them, as we see from the corresponding transmission image. Therefore, stimulated emission microscopy opens up the possibility of visualizing chromoproteins that are not accessible by fluorescence microscopy.

Next, we show the stimulated emission imaging in live *E. coli* cells of a non-fluorescent indigo reaction product commonly used to assay gene expression. β-galactosidase catalyses the cleavage of the glycosidic linkage of X-gal, a popular chromogenic substrate, eventually forming an indigo product after oxidation[21]. The gene encoding β-galactosidase, *lacZ*, is a classic reporter gene. Traditionally, the indigo product has to accumulate in sufficient concentration for its blue colour to be visible[21]. With stimulated emission, the accumulation of the indigo product can now be monitored in wild-type cells without induction of *lacZ* (Fig. 3e–g). The inhomogeneous distribution of the indigo product inside individual cells (Fig. 3e and f) is consistent with the fact that the product is insoluble and tends to form localized precipitates. In contrast, the corresponding transmission image (Fig. 3g) shows no signs of any colour. Although an assay using a fluorogenic substrate has recently been developed[22], it requires microfluidics to enclose individual cells because the hydrolysis product there is quickly pumped out by the cell. Hence, stimulated emission microscopy allows us to monitor a product that is assumed to report basal *lacZ* gene activity with superb sensitivity.

Monitoring transdermal delivery of non-fluorescent drug with intrinsic three-dimensional optical sectioning is another application. In particular, we show mapping of a cationic thiazine dye toluidine blue O (TBO) at both the cellular and tissue levels. Having a selective affinity for cancer cells *in vivo*, TBO is a photosensitizer in photodynamic

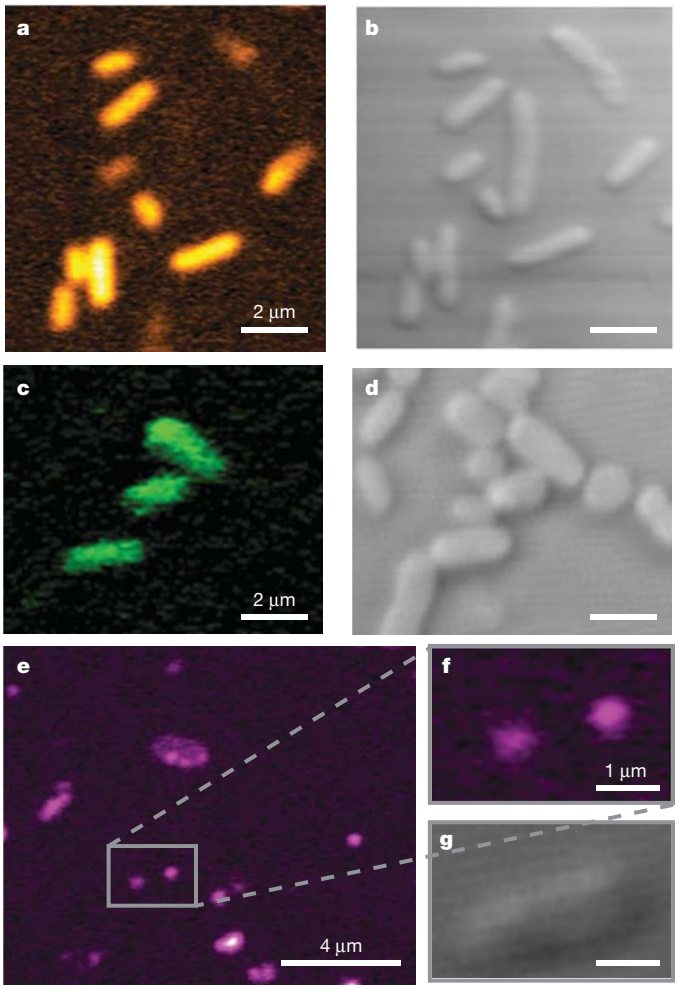

Figure 3 | Imaging non-fluorescent chromoproteins and chromogenic reporter for gene expression. Imaging distributions of cytoplasmic chromoproteins gtCP (**a**) and cjBlue (**c**) in live *E. coli* cells, respectively, by stimulated emission microscopy. **b** and **d** are the corresponding wide-field transmission images. Plasmids containing the genes encoded for gtCP and cjBLue are transformed into *E. coli*, respectively. cjBlue is expressed less abundantly than gtCP inside cells. **e**, Stimulated emission imaging of the oxidation product (4,4′-dichloro-5,5′-dibromoindigo) resulting from X-gal hydrolysis catalysed by β-galactosidase, the protein encoded by the *lacZ* reporter gene. Indigo accumulation in *E. coli* cells is detected without any *lacZ* induction. The signal is detected only when both the cells and X-gal are present. Unlike the homogeneous protein images in **a** and **c**, the indigo product shows inhomogeneous localized distribution inside cells owing to its insolubility, as shown in the magnified image **f**. The direct transmission image **g** shows the morphology of the same region. gtCP and cjBlue absorb around 580 nm (ref. 18) and 610 nm (ref. 19), respectively; indigo product has a broad absorption of 600 to 650 nm. Wavelengths for excitation and stimulation, respectively, are 590 nm and 660 nm in **a** and **c**, and 600 nm and 680 nm in **e** and **f**. The excitation and stimulation beams of 0.1 mW and 0.3 mW, respectively, and time delay of ~0.3 ps are used for all the above images. All of the images were taken between 5 s and 45 s, depending on the image size.

therapy[23,24]. Subcellular localization of TBO is crucial because it influences both the level and the kinetics of apoptosis induction. However, it is difficult to image the true TBO distribution, because its fluorescence is quenched when bound to tissue substrates and only the non-specific stain residue in the tissue retains its native fluorescence[24]. Independent of the complication from fluorescence contrast, stimulated emission microscopy is suitable for this problem. The stimulated emission image of TBO inside the cancer cells after incubation shows its local accumulation (Supplementary Fig. 1). When topically applied to skin tissue, being hydrophilic and water soluble, TBO is enriched in the centre of the protein phase of the polygonal *stratum corneum* cells rather than in the intercellular space which is in the lipid phase (Fig. 4a). At a level 20 μm deeper, TBO displays a rich subcellular distribution in the cytoplasm of the epidermis, where cellular proliferation actively takes place (Fig. 4b). These imaging results support the hydrophilic delivery pathway as well as the recent hypothesis that TBO binds to cytoplasmic RNA to initiate apoptosis[23].

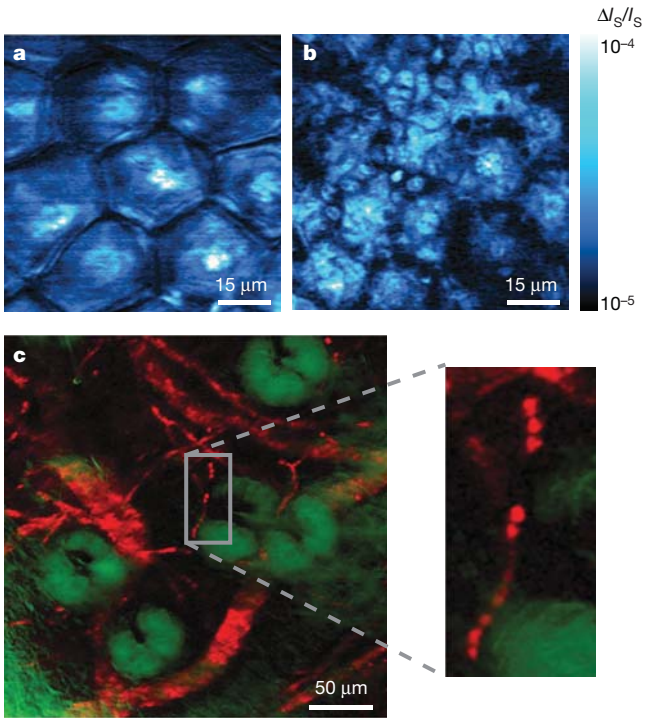

Figure 4 | Transdermal drug distribution in three-dimensional and microvascular imaging. a, **b**, Drug delivery of TBO, a drug used as photosensitizer in photodynamic therapy, to the same area of freshly cut mouse ear skin at two different depths (3 μm and 25 μm), 30 min after topical application of 10 μM TBO/PBS solution. At the surface layer (3 μm) of *stratum corneum*, **a** shows TBO accumulated in the protein phase of the polygonal cells rather than in the lipid-rich intercellular space. At the layer of epidermis (25 μm), **b** shows a rich TBO distribution following the subcellular cytoplasm of nucleated basal keratinocytes. These images support the 'hydrophilic path' as a main pathway for transdermal drug delivery of TBO. Wavelengths are 600 nm and 680 nm for excitation and stimulation, respectively. The excitation and stimulation beams have 0.1 mW and 0.3 mW, respectively, at the focus, and the time delay is ~0.3 ps. The colour table (cyan indicates hot) shows the magnitude of $\Delta I_S/I_S$. **c**, *Ex vivo* imaging of microvasculature network of a mouse ear based on endogenous haemoglobin contrast. The stimulated emission image (red channel, maximum intensity projection) shows the blood vessel network surrounding sebaceous glands (green channel, simultaneously recorded by confocal reflectance). In the zoomed-in image, individual red blood cells are lined up within a single capillary (~5 μm in diameter). In **c**, 830 nm (~20 mW) and 600 nm (~3 mW) are used for two-photon excitation of Soret band and one-photon stimulated emission of *Q* band of haemoglobin, respectively. Pulse widths of both excitation and stimulation beams are about 0.2 ps with a ~0.2 ps time delay between them.

Finally, we demonstrate label-free imaging of microvascular structure, based on endogenous contrast from non-fluorescent haemoglobin. The structure and haemodynamics of blood vessels play a major role in many biomedical processes, such as angiogenesis in tumours[25] and cerebral oxygen delivery in the brain[26,27]. However, established techniques such as magnetic resonance imaging, computed tomography, positron emission tomography, ultrasound, confocal and two-photon fluorescence microscopy either lack the spatial resolution needed to resolve individual capillaries or require exogenous contrast agents. Here we perform *ex vivo* stimulated emission imaging of the well-developed vascular network from a nude mouse ear, by exciting the Soret band of haemoglobin through efficient two-photon absorption[28] and subsequently stimulating the emission from its *Q* band, which has a longer excited-state lifetime than the Soret band[29]. As shown in Fig. 4c, blood vessels (in red) branch and loop around sebaceous glands (in green). In addition, single red blood cells can be clearly seen to reside within individual capillaries (~5 μm in diameter). Two-photon absorption has recently been developed to image haemoglobin[13]. We note that stimulated emission is more sensitive because it involves direct one-photon transition. Furthermore, our new technique offers the prospect of three-dimensional mapping of blood oxygenation levels to address a broad range of physiological and pathological problems[25–27].

We note that the complexity and cost of the instrument can be much reduced as fibre laser sources are adapted. Stimulated emission microscopy allows imaging of non-fluorescent chromophores with three-dimensional optical sectioning and high sensitivity, and extends the repertoire of reporters for biological imaging beyond fluorophores.

METHODS SUMMARY

In the scheme depicted in Fig. 1, two femtosecond optical parametric oscillators (Coherent/APE) are synchronously pumped by a femtosecond mode-locked 76-MHz Ti:sapphire laser (Coherent). Two independent frequency-doubled outputs from these two optical parametric oscillator signal waves, in the wavelength range of 560 to 700 nm with pulse widths around 200 fs, serve as excitation and stimulation pulse trains. A pulse compressor consisting of a pair of SF11 prisms is built to control the pulse width. Collinear excitation and stimulation beams are combined and focused with a high numerical aperture (NA = 1.2) objective onto a common focal spot. The temporal delay between the synchronized excitation and stimulation inter-pulse is adjusted to between 0.2 and 0.3 ps. The intensity of the excitation beam is modulated by an acousto-optical modulator (Crystal technology) at 5 MHz. A condenser with NA = 0.9 is used to collect the forward propagating stimulation beam, which is spectrally filtered before being detected by a photodiode. To acquire images with a laser scanning microscope (FV300, Olympus), we used a 100-μs time constant for a lock-in amplifier (SR844, Stanford Research) and pixel dwell time of 190 μs.

Received 28 March; accepted 13 August 2009.

1. Pawley, J. B. (ed.) *Handbook of Biological Confocal Microscopy* 3rd edn (Springer, 2006).
2. Lakowicz, J. R. *Principles of Fluorescence Spectroscopy* (Plenum Press, 1983).
3. Turro, N. J. *Modern Molecular Photochemistry* (University Science Books, 1991).
4. Einstein, A. On the quantum theory of radiation. *Phys. Z.* **18**, 121 (1917).
5. Seigman, A. E. *Laser* 264–307 (University Science Books, 1986).
6. Hamilton, C. E., Kinsey, J. L. & Field, R. W. Stimulated emission pumping: new methods in spectroscopy and molecular dynamics. *Annu. Rev. Phys. Chem.* **37**, 493–524 (1986).
7. Hell, S. W. & Wichmann, J. Breaking the diffraction resolution limit by stimulated emission: stimulated-emission-depletion fluorescence microscopy. *Opt. Lett.* **19**, 780–782 (1994).
8. Dong, C. Y., So, P. T., French, T. & Gratton, E. Fluorescence lifetime imaging by asynchronous pump-probe microscopy. *Biophys. J.* **69**, 2234–2242 (1995).
9. Cantor, C. R. & Schimmel, P. R. *Biophysical Chemistry* 361–374 (W. H. Freeman, 1980).
10. Moerner, W. E. & Kador, L. Optical detection and spectroscopy of single molecules in a solid. *Phys. Rev. Lett.* **62**, 2535–2538 (1989).
11. Ye, J., Ma, L. S. & Hall, J. L. Ultrasensitive detections in atomic and molecular physics: demonstration in molecular overtone spectroscopy. *J. Opt. Soc. Am. B* **15**, 6–15 (1998).
12. Freudiger, C. W. *et al.* Label-free biomedical imaging with high sensitivity by stimulated Raman scattering microscopy. *Science* **322**, 1857–1861 (2008).

13. Fu, D. *et al.* High-resolution *in vivo* imaging of blood vessels without labeling. *Opt. Lett.* **32,** 2641–2643 (2007).
14. Denk, W., Strickler, J. H. & Webb, W. W. Two-photon laser scanning fluorescence microscopy. *Science* **248,** 73–76 (1990).
15. Evans, C. L. & Xie, X. S. Coherent anti-Stokes Raman scattering microscopy: chemical imaging for biology and medicine. *Annu. Rev. Anal. Chem.* **1,** 883–909 (2008).
16. Rittweger, E., Rankin, B. R., Westphal, V. & Hell, S. W. Fluorescence depletion mechanisms in super-resolving STED microscopy. *Chem. Phys. Lett.* **442,** 483–487 (2007).
17. Du, H. *et al.* PhotochemCAD: A computer-aided design and research tool in photochemistry. *Photochem. Photobiol.* **68,** 141–142 (1998).
18. Gurskaya, N. G. *et al.* GFP-like chromoproteins as a source of far-red fluorescent proteins. *FEBS Lett.* **507,** 16–20 (2001).
19. Chan, M. C. Y. *et al.* Structural characterization of a blue chromoprotein and its yellow mutant from the sea anemone *Cnidopus japonicus*. *J. Biol. Chem.* **281,** 37813–37819 (2006).
20. Zhang, J., Campbell, R. E., Ting, A. Y. & Tsien, R. Y. Creating new fluorescent probes for cell biology. *Nature Rev. Mol. Biol.* **3,** 906–918 (2002).
21. Miller, J. H. *Experiments in Molecular Genetics* 171–224 (Cold Spring Harbor Laboratory, 1972).
22. Cai, L., Friedman, N. & Xie, X. S. Stochastic protein expression in individual cells at the single molecule level. *Nature* **440,** 358–362 (2006).
23. Tremblay, J. F. *et al.* Photodynamic therapy with toluidine blue in Jurkat cells: cytotoxicity, subcellular localization and apoptosis induction. *Photochem. Photobiol. Sci.* **1,** 852–856 (2002).
24. Chelvanayagam, D. K. & Beazley, L. D. Toluidine blue-O is a Nissl bright-field counterstain for lipophilic fluorescent tracers Di-ASP, DiI and DiO. *J. Neurosci. Methods* **72,** 49–55 (1997).
25. McDonald, D. M. & Choyke, P. L. Imaging of angiogenesis: from microscope to clinic. *Nature Med.* **9,** 713–725 (2003).
26. Grinvald, A., Lieke, E., Frostig, R. D., Gilbert, C. D. & Wiesel, T. N. Functional architecture of cortex revealed by optical imaging of intrinsic signals. *Nature* **324,** 361–364 (1986).
27. Kleinfeld, D., Mitra, P. P., Helmchen, F. & Denk, W. Fluctuations and stimulus-induced changes in blood flow observed in individual capillaries in layers 2 through 4 of rat neocortex. *Proc. Natl Acad. Sci. USA* **95,** 15741–15746 (1998).
28. Clay, G. O., Schaffer, C. B. & Kleinfeld, D. Large two-photon absorptivity of hemoglobin in the infrared range of 780–880 nm. *J. Chem. Phys.* **126,** 025102 (2007).
29. Wang, W. *et al.* Femtosecond multicolor pump-probe spectroscopy of ferrous cytochrome c. *J. Phys. Chem. B* **104,** 10789–10801 (2000).

Supplementary Information is linked to the online version of the paper at www.nature.com/nature.

Acknowledgements We thank K. Lukyanov and A. Miyawaki for the gifts of chromoprotein gtCP and cjBlue plasmid DNA, respectively; Coherent Inc. for lending us a femtosecond optical parametric oscillator; and P. Choi for preparing X-gal *E. coli* cells. We also thank B. G. Saar, C. W. Freudiger, S. Basu, J. W. Lichtman and C. B. Schaffer for discussions, and R. Tsien for suggesting the use of chromoproteins. This work was supported by a National Science Foundation (grant CHE-0634788) and the US Department of Energy's Basic Energy Sciences Program (DE-FG02-07ER15875).

Author Contributions W.M., S.L. and S.C. performed experiments and analysed data. R.R. constructed *E. coli* cells expressing chromoproteins. G.R.H. and S.C. helped to construct the laser systems. W.M., S.L. and X.S.X. conceived the concept, designed the experiments and wrote the paper.

Author Information The authors declare competing financial interests: details accompany the full-text HTML version of the paper at www.nature.com/nature. Reprints and permissions information is available at www.nature.com/reprints. Correspondence and requests for materials should be addressed to X.S.X. (xie@chemistry.harvard.edu).